13th International Conference on Greenhouse Gas Control Technologies, GHGT-13, 14-18 November 2016, Lausanne, Switzerland

COMPOSITE: A concept for high efficiency power production with integrated CO_2 capture from solid fuels

Yngve Larring[a]*, Schalk Cloete[a], Antonio Giuffrida[b], Matteo C. Romano[b], Paolo Chiesa[b], John Morud[a], Mehdi Pishahang[a], Actor Chikukwa[a], Shahriar Amini[a], Andrew Tobiesen[a]

*a*SINTEF Materials and Chemistry, P.O. Box 4760 Sluppen, NO-7465 Trondheim, Norway
*b*Politecnico di Milano, Department of Energy, Via Raffaele Lambruschini 4, Milano 20156, Italy

Abstract

The COMPOSITE concept combines packed bed chemical looping combustion (PBCLC) with chemical looping for oxygen production (CLOP) in an integrated gasification combined cycle for high efficiency power production. Detailed reactor modelling of the PBCLC and CLOP reactors was combined with process and power cycle modelling for the COMPOSITE plant in order to estimate the electric efficiency and CO_2 avoidance. The efficiency of the COMPOSITE process amounted to 45.3% compared to 40.5-42% for the PBCLC-IGCC process and 37.7% for pre-combustion IGCC, with a CO_2 capture efficiency of about 95%.

1. Introduction

The COMPOSITE concept is based on an integrated gasification combined cycle (IGCC) including a novel CLOP (Chemical Looping Oxygen Production) – EPCG (Enhanced Pressurized Coal Gasification) – CLC (Chemical

---

* Corresponding author. Tel.: +4798283956
  E-mail address: Yngve.Larring@sintef.no

Looping Combustion) system for efficient combustion of solid fuel with inherent CO_2 capture. This process is described in more detail in the next section (Figure 1).

Oxygen production represents an important energy penalty in IGCC power plants, reducing electric efficiency by about 4 %-points when using conventional cryogenic air separation. Other oxygen production methods have been tested such as Ceramic Autothermal Recovery (CAR) [1] and Chemical Looping Air Separation (CLAS) [2], but since the large amount of heat at moderate temperature in the waste gases cause additional efficiency losses for these systems, they do not achieve much gain in performance. The COMPOSITE concept has the advantage of utilizing the lean semi-hot air from the CLOP process for heat removal in a fixed bed PBCLC, thus increasing the heat content and reducing the energy penalty associated with oxygen production.

The concept also includes hot gas cleaning (around 400 °C) which reduces the penalties compared to traditional scrubbing. As a matter of fact, based on a previous work of the authors [3], up to 2.5% improvement in IGCC efficiency seems to be possible when switching from cold to hot coal-derived gas clean-up. The materials used in the CLOP and PBCLC will also have a longer lifetime since the degree of reduction and temperature cycling is reduced compared a PBCLC-IGCC plant. Furthermore, the material is not exposed to attrition and to ashes and elements in coal that can give a reduced lifetime like in CLC of coal in fluidized bed. The demands on material strength though is of high importance in this concept.

1.1. IGCC power plant configurations with CO_2 capture

The IGCC power plant configuration lends itself well to pre-combustion CO_2 capture, resulting in an electric efficiency of 37.7% with 87% CO_2 avoidance when future advanced gas turbine technology is employed [4, 5]. Significant improvements on these numbers can be achieved by carrying out syngas combustion via FBCLC in order to achieve inherent CO_2 separation with minimal energy penalty. For example, electric efficiencies of 40.5-42% and CO_2 avoidance over 95% can be achieved when packed or circulating fluidized bed CLC configurations are integrated into an IGCC power plant [4, 6].
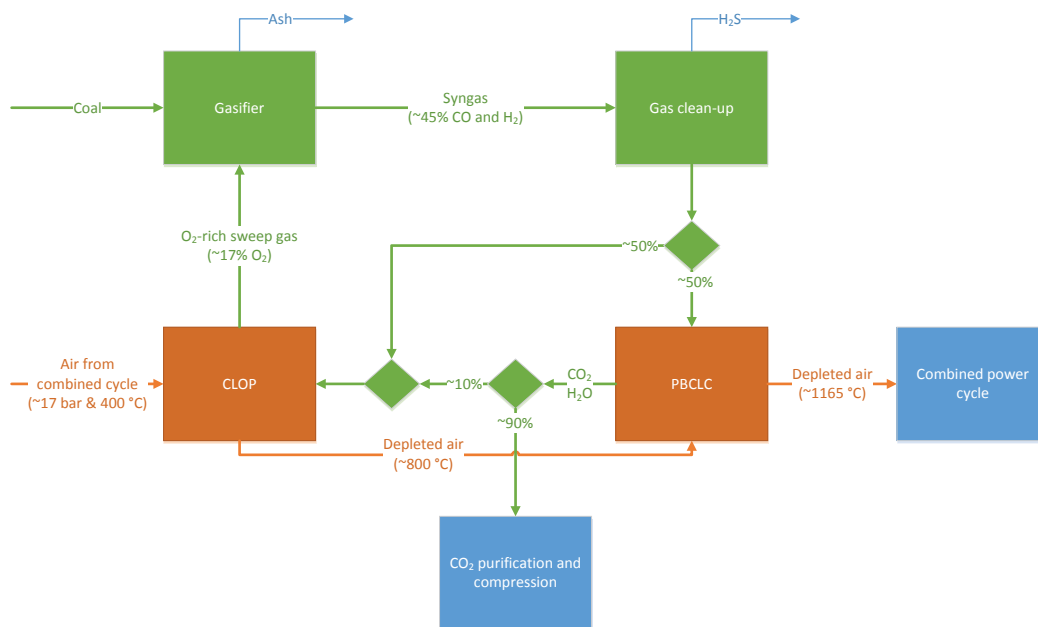

Figure 1: Schematic diagram of the COMPOSITE process. Green process streams contain carbon, while orange process streams contain nitrogen. Inherent separation of these streams is ensured in the CLOP and PBCLC units (orange).

An equivalent of about 4 %-points of efficiency is lost through the need to employ an air separation unit (ASU) to supply oxygen to the gasifier. The COMPOSITE process addresses this energy penalty by replacing the ASU with a CLOP unit, which is efficiently integrated into the process configuration (Figure 1).

The CLOP unit displaces the ASU unit by supplying a stream of 17% O_2 (the balance is CO_2 and H_2O) to the gasifier. Normally, this would result in a significant energy penalty because of the large quantity of air that needs to be heated up to the CLOP process temperature. In the COMPOSITE configuration, however, this large air stream is efficiently utilized in the PBCLC unit where it is further heated to temperatures suitable for power production in a combined cycle. This configuration holds an additional advantage if low-cost natural minerals are used as the oxygen carrier in the PBCLC reactors.

Under normal PBCLC-IGCC operation, a large recycle stream of N_2 is required to remove the heat from the system so that reduction can take place directly after oxidation (when the reactor temperature is high) [7]. If reduction is carried out before oxidation, the low reactor temperature (~400 °C) will result in incomplete reduction and lots of fuel slip. In the COMPOSITE process, however, reduction can be carried out before oxidation since the cooling temperature of the gases coming from the CLOP unit at ~800 °C is sufficient for reduction. This avoids the need for a N_2 recycle stream and the associated capital costs (and complexity) from a N_2 recycle cooling system and a gas cycle compressor with a higher inlet temperature and volume flow rate.

The relatively low O_2 concentration in the stream entering the gasifier results in a syngas with a lower heating value (~45% less) compared to the use of an ASU. This will result in larger gasification and gas clean-up units and increase the energy penalty associated with cooling of the syngas for gas clean-up and boosting to overcome the pressure drops in the reactors. On the other hand, the high CO_2 and H_2O content of the syngas will prevent carbon deposition on the oxygen carrier saving a potentially significant energy penalty associated with syngas dilution [4]. In addition, no steam is required in the gasifier because of the large amounts of CO_2 and H_2O entering with the O_2 from the CLOP unit.

The effect of these trade-offs will be quantified in this paper by determining the overall electric efficiency that can be achieved by the COMPOSITE plant and benchmarking it against the PBCLC and pre-combustion IGCC configurations.

Nomenclature

α	Volume fraction
ρ	Density (kg/m^3)
d_{gr}	Grain diameter (m)
k	Reaction rate constant
M	Molar weight (kg/mol)
N	Number of moles (mol)
n	Reaction order
P	Pressure (bar)
R	Ideal gas constant (J/mol.K)
R^H	Heterogeneous reaction rate (mol/m^{3}s)
s	Active surface area fraction
T	Temperature (K)
t	Time (s)
V	Volume (m^3)
w_{ox}	Degree of oxidation
w_{red}	Degree of reduction
X	Conversion
x	Mole fraction
Y	Mass fraction

Subscripts
eq   Equilibrium
i   Species index
s   Solids

Abbreviations
CLC   Chemical looping combustion
CLOP   Chemical looping oxygen production
HGCU   Hot gas clean-up
HRSG   Heat recovery steam generator
HT, HP High temperature, high pressure
IGCC   Integrated gasification combined cycle
IP   Intermediate pressure
PBCLC   Packed bed chemical looping combustion
TOT   Turbine outlet temperature

2. Reactor simulations

The two most novel units in the COMPOSITE concept, the CLOP and PBCLC packed bed reactors, will be simulated in more detail using 1D modelling. An Eulerian multifluid approach was used where the solids phase velocity was set to zero. Details of the approach can be found in an earlier publication [8]. Kinetics of the PBCLC reactor using an Ilmenite oxygen carrier can also be found in the aforementioned work (including mass transfer limitations and inverse pressure dependency), but kinetics for the CLOP process will be described in more detail below.

2.1. CLOP kinetics

Due to the novelty of the CLOP process, detailed kinetic models are not yet available in the literature. For this reason, a preliminary model was derived from TGA experiments for this modelling study using a $Ca_2AlMnO_{5.5}$ material (henceforth abbreviated as CAM). The largest uncertainty is related to the kinetic behavior when approaching the equilibrium oxygen concentration. This has not been determined experimentally, but a conservative assumption has been made that the reaction rate increases linearly from zero at equilibrium to a maximum when the actual oxygen mole fraction deviates by 0.1 from the equilibrium oxygen mole fraction.

$$R_{O_2}^H = -\frac{1}{V}\frac{dN_{O_2}}{dt} = \begin{cases} 7.7\times10^{10}\, e^{\left(\frac{-174500}{RT}\right)} w_{ox}^{2/3} \min\left(10\left(x_{O_2}-x_{O_2,eq}\right),-1\right) & \text{if } \left(x_{O_2}-x_{O_2,eq}\right) \leq 0 \\ 27 w_{red}^{2/3} \max\left(10\left(x_{O_2}-x_{O_2,eq}\right),1\right) & \text{if } \left(x_{O_2}-x_{O_2,eq}\right) > 0 \end{cases} \qquad \text{Equation 1}$$

The equilibrium O_2 mole fraction was approximated using the Van't Hoff relation using the reaction enthalpy and one reference point for oxygen partial pressure and temperature. The reaction enthalpy was estimated based on TG experiments to be 91 kJ/mol and a reference temperature of 720 °C at an oxygen partial pressure of 1 bar was determined from TGA studies, resulting in the following equation:

$$x_{O_2,eq} = \frac{1}{P}\exp\left(\frac{-91000}{R}\left(\frac{1}{T}-\frac{1}{993.15}\right)+\log\left(1\right)\right) \qquad \text{Equation 2}$$

In addition, a region of CuO oxygen carrier was introduced in the initial region of the reactor to combust the CO and H_2 in the incoming gases to raise the CLOP reactor temperature to acceptable levels. It is possible that the CAM material can also be directly reduced by CO and H_2, but this has not been experimentally tested and no kinetic data is available. CuO is known to be highly reactive to reduction with syngas even at low temperature and is therefore included in this study. The following reaction rate is implemented:

$$R_i^H = -\frac{1}{V}\frac{dN_i}{dt} = \frac{6}{d_{gr}} s \left(1-X\right)^{2/3} \alpha_s k \left(\frac{Y_i \rho_g}{M_i}\right)^n$$

Equation 3

The active surface area in the Cu particle $\left(s\right)$ is 0.1, the grain diameter $\left(d_{gr}\right)$ is 0.8 nm in diameter for reduction and 0.52 nm in diameter for oxidation, and the reaction orders $\left(n\right)$ for the reactions involving H_2, CO, CH_4 and O_2 are 0.6, 0.8, 0.4 and 1 respectively [9]. The reaction rate constants $\left(k\right)$ for different reactions are taken from Abad et al. [9, 10], which found that an increase in pressure reduced the reaction rate constant:

$$k_{H_2} = \frac{1\times10^{-4}}{P^{0.53}} e^{\left(\frac{-33000}{RT}\right)}$$

$$k_{CO} = \frac{5.9\times10^{-6}}{P^{0.83}} e^{\left(\frac{-14000}{RT}\right)}$$

Equation 4

$$k_{CH_4} = 4.5\times10^{-4} e^{\left(\frac{-60000}{RT}\right)}$$

$$k_{O_2} = \frac{4.7\times10^{-6}}{P^{0.68}} e^{\left(\frac{-15000}{RT}\right)}$$

The mass transfer limitation model presented in an earlier work [11] was also applied to these reactions.

2.2. Geometry, materials and boundary conditions

A simple 1D geometry, 10 m in length, was created for both reactors and meshed with 100 cells. This mesh was sufficient to resolve the reaction and heat fronts moving through the packed bed reactor.

The beds were packed with 5 mm particles. The CAM material consisted of three species: $Ca_2AlMnO_{5.5}$ (oxidized), Ca_2AlMnO_5 (reduced) and an inert Ca_2AlMnO_5 which comprised a mass fraction of 0.25 because the TGA results which showed that the oxygen carrying capacity of the material was only 75% of the theoretical maximum. The densities of $Ca_2AlMnO_{5.5}$ and Ca_2AlMnO_5 were 2067 and 2000 kg/m^3 respectively. The Cu-based oxygen carrier consisted of CuO (oxidized) with a density of 2799 kg/m^3, Cu (reduced) with a density of 3842 kg/m^3 and an alumina support with a density of 1714 kg/m^3. An active content of 15% was assumed in order to limit the maximum temperature in the material to 950 °C. Lastly, ilmenite was assumed to consist of Fe_2O_3 (oxidized) with a density of 3144 kg/m^3, FeO (reduced) with a density of 2829 kg/m^3 and inert TiO_2 with a density of 2538 kg/m^3. An active content of 19.6% was set to limit the maximum reactor temperature to 1200 °C. The ideal gas law was implemented for calculated gas densities. Heat capacities were implemented as a function of temperature based on the correlations of Robie [12] for the solids and on JANAF thermochemical tables [13] for the gas. The heat capacity of the CAM material was approximated by averaging the heat capacity of three similar materials: $CaFe_2O_5$, $Ca_2Ti_2O_5$ and $CaTiO_3$ from based on data from FactSage™ a thermodynamic software.

Boundary conditions for the two reactors were derived from a preliminary process simulation in order to maximize accuracy. The CLOP reactor receives compressed air during the oxidation stage and a mix of syngas from gas clean-up and combustion products from the PBCLC unit. Details are given in Table 1.

Table 1: CLOP reactor inlet streams.

Stream	Stage time (s)	Mass flux (kg/m²s)	Temperature (°C)	Composition (mole fraction)	
Oxidation	360	5.5	404.4	O_2	0.2073
				H_2O	0.0103
				CO_2	0.0003
				Ar	0.0092
				N_2	0.7729
Reduction	60	3.54	514.1	H_2	0.1085
				CO	0.3252
				CH_4	0.0170
				H_2O	0.1705
				CO_2	0.3714
				N_2	0.0075

The PBCLC reactors receive a heated stream depleted air from the CLOP reactors during the oxidation stage and fuel from the gas clean-up unit during the reduction stage. These two streams are specified in Table 2.

Table 2: PBCLC reactor inlet streams.

Stage	Stage time (s)	Mass flux (kg/m²s)	Temperature (°C)	Composition (mole fraction)	
Oxidation	1500	4.6	800	O_2	0.1642
				H_2O	0.0109
				CO_2	0.0003
				Ar	0.0097
				N_2	0.8149
Reduction	300	2.55	432.2	H_2	0.1184
				CO	0.3549
				CH_4	0.0185
				H_2O	0.1584
				CO_2	0.3423
				N_2	0.0075

Mass fluxes for both reactors were specified to result in superficial gas velocities in the order of 1 m/s, which should result in a reasonable trade-off between reactor cross sectional area and pressure drop. The reduction stage of the PBCLC reactor has a slower superficial velocity to ensure complete conversion of the material.

2.3. Solver settings

The commercial CFD package, FLUENT 16.1 was used as the flow solver to carry out the simulations. The phase-coupled SIMPLE algorithm [14] was selected for pressure-velocity coupling, while the QUICK scheme [15] was employed for discretization of all remaining equations. 2nd order implicit temporal discretization was used.

3. The power plant

The power plant simulated in this work is based on an integration of the previously detailed reactors with a gasification island and a power island, the latter consisting of a combined cycle. As schematized in Figure 2, the gasification system, based on the high-temperature Winkler concept [16], is fed by a charge of bituminous coal, loaded via a stream of separated and compressed CO_2. The gasifier delivers syngas at 900°C, which is cooled to 400°C by HP steam production and superheating. Sulfur species are removed in a hot gas desulfurization unit at 400°C by means of a zinc-based sorbent process based on interconnected transport reactors [17]. The process integration of hot gas desulfurization process in IGCCs has been thoroughly investigated by the authors in the past [18, 19], as a solution to improve the power plant performance. High temperature desulfurization process is particularly promising in this application because the cooling to nearly ambient temperature of the very large syngas flow rate obtained with the proposed gasification process would cause major energy penalty and high capital cost. The sulfur-free syngas is then boosted to the CLOP and CLC reactors.

Along with the syngas cooler present at the exit of the gasifier, two other main heat exchange sections are included in the plant.

- A HT CO_2 cooler is included at the exit of the CLC system for heat recovery from the CO_2-rich stream, used for (i) HP steam production and superheating (at 565°C), (ii) completing IP steam reheating and HP steam superheating initiated in the heat recovery steam generator. The tail-end CO_2-rich stream is further cooled down to nearly ambient temperature by economizing HP water.
- A three-level (144, 36 and 4 bar) heat recovery steam generator (HRSG) is present for heat recovery from the gas turbine exhaust gas. However, considering the gas turbine outlet temperature (TOT) of around 510°C (stream 18), HP superheating and IP reheating are completed outside the HRSG, in the HT exhaust cooler, as previously anticipated.

A smaller heat exchanger is also present to cool the solid by-products exiting the bottom of the gasifier down to 300°C, with IP steam production.

Regarding the turbomachinery in the power plant, a large-size gas turbine is used for the topping cycle, with a pressure ratio of 17 at the compressor and a turbine inlet temperature of 1165°C (stream 17).

The in-house code GS has been used for the calculation of the plant mass and energy balances. The use of GS is mainly justified by the capability of reliably calculating cooled gas turbines by a built-in model [20], based on a stage-by-stage calculation approach which takes into account the blade cooling needs and has been successfully used in past works to calculate a variety of IGCC plant configurations [21-23]. The assumptions for power plant component simulation are consistent with the ones adopted in a previous work by the authors [4].
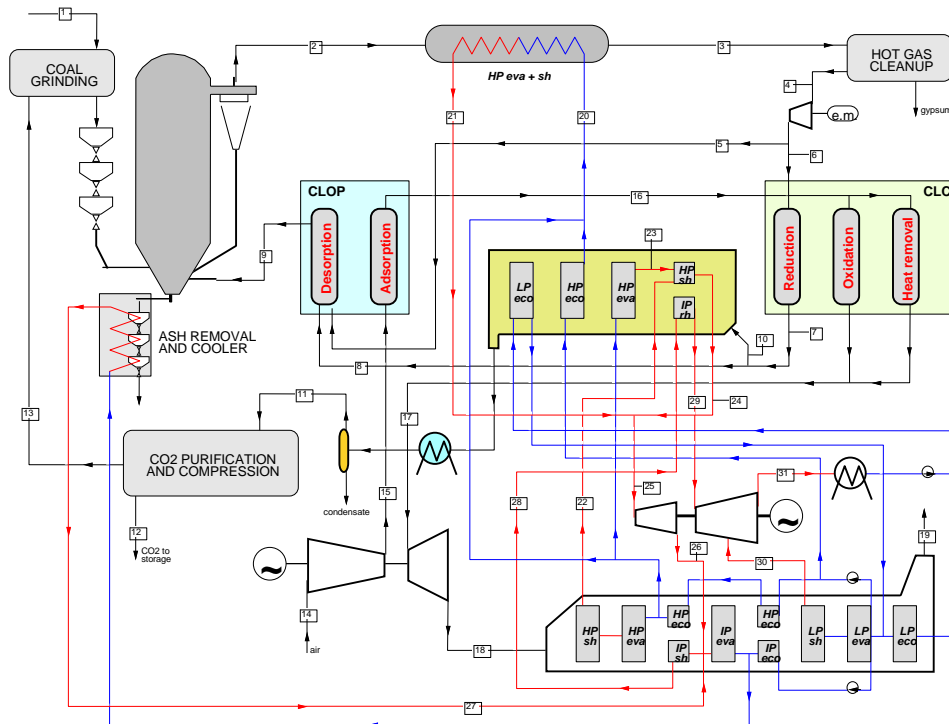

Figure 2: Scheme of the power plant.

4. Reactor simulation results

4.1. CLOP reactor

The transient operation of the CLOP reactor is discussed below based on the four contour plots in Figure 3.
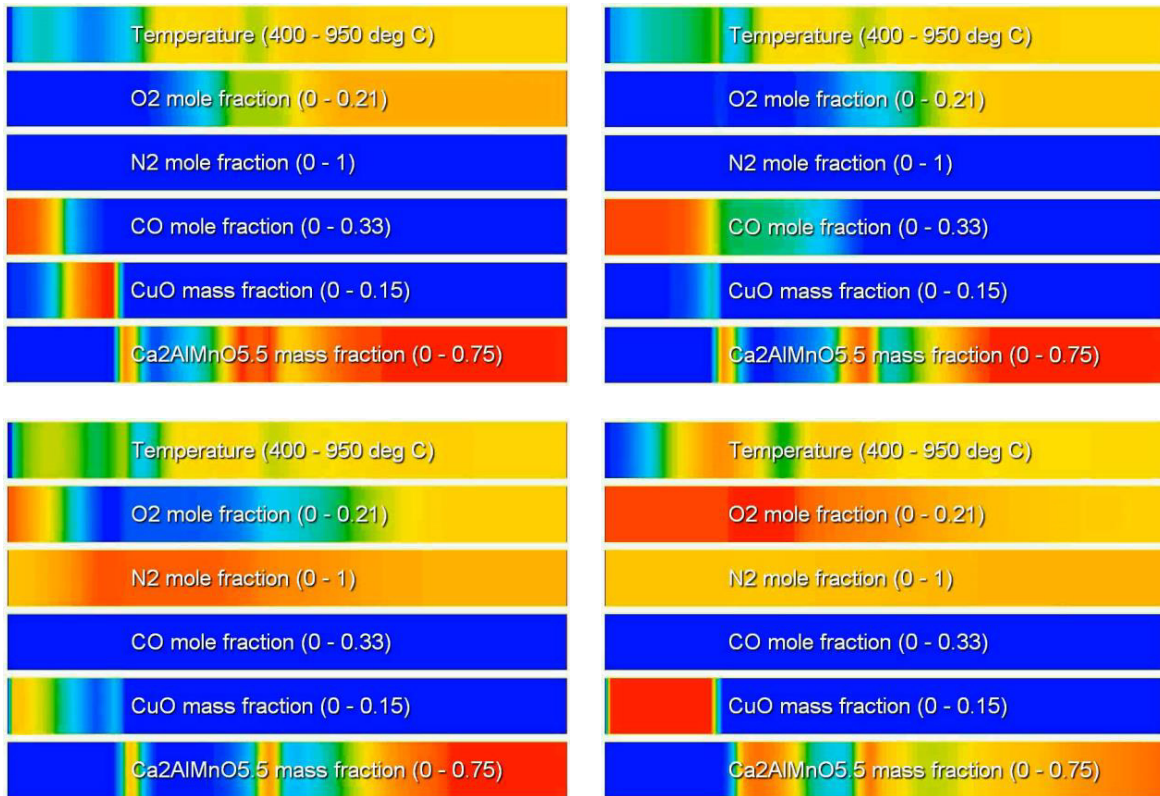
Figure 3: Contour plots illustrating CLOP operation (flow from left to right through the domain). The top two images show the middle and end of the reduction stage and the bottom two images show the initial stages and middle of the oxidation stage. Numbers in brackets on each contour plot indicate the range on the blue-green-red colourmap where the low number represents blue and the high number represents red. Note that $Ca_2AlMnO_{5.5}$ is the oxidized state of the CAM material and CuO is the oxidized state of the Cu-based oxygen carrier.

The top two images of Figure 3 (reduction stage) clearly illustrates the function of the CLOP reactor: separation of oxygen and nitrogen. Both images show high oxygen concentrations at the reactor outlet, but no nitrogen. The top left image also illustrates the function of the Cu-based oxygen carrier in the initial part of the reactor: combusting the fuel gases. This can be seen from the reaction front of CO reducing CuO. The temperature in the initial part of the reactor is increased by this exothermic reaction. At the end of the reduction stage (top right), some CO slips past the CuO and reacts with the free oxygen released from the CAM material.

Oxygen release from the CAM material can only take place when the local oxygen mole fraction is lower than the equilibrium mole fraction at a given temperature. This reaction therefore takes place in regions of low oxygen mole fractions and high temperatures (the equilibrium oxygen partial pressure increases with temperature according to Equation 2). Closer inspection of the top two images in Figure 3 shows that these conditions are met in the central regions of the reactor, leading to some oxygen release.

The initial part of the oxidation stage (bottom left image in Figure 3) shows the oxidation front moving through the Cu-based material at the start of the bed. This oxidation reaction consumes all the incoming oxygen and all oxygen still visible towards the outlet of the reactor is released by the CAM material. When the Cu-based material is completely oxidized (bottom right image in Figure 3), the local oxygen mole fraction can exceed the equilibrium mole fraction and the CAM material can once again be oxidized. As the oxidation stage continues and the reactor is heated up by the exothermic oxidation reaction, the equilibrium oxygen mole fraction also increases, implying that only a small fraction of the incoming oxygen can react. This requires a very long oxidation stage, which can be

afforded in the COMPOSITE concept because the hot depleted air stream emerging from this stage is directly utilized in the PBCLC reactors (see Figure 1).

Figure 4 gives outlet species and temperature profiles for the CLOP reactor. The separation of oxygen from nitrogen during the reduction stage (first 60 s) is clearly visible. It is also clear that the nitrogen concentration at the outlet does not drop immediately at the start of the reduction stage, but shows a ~7 s lag time as it is purged out of the reactor by the incoming reduction gases. Since the reduction stage is only 60 s long in this case, significant mixing of N_2 and CO_2 will occur if the outlet gases are switched at the same time as the inlet gases. For this reason, a 7 s time delay between the inlet switch and the outlet switch is implemented. In this case, the separation between the reduction and oxidation streams is very good due to the plug flow nature of the packed bed reactor. Separation efficiency amounted to 98.9%, implying that 1.1% of the reduction stage outlet gas exits during the oxidation stage and is replaced by gases from the oxidation stage. This will slightly reduce the CO_2 capture efficiency and CO_2 purity from the process.
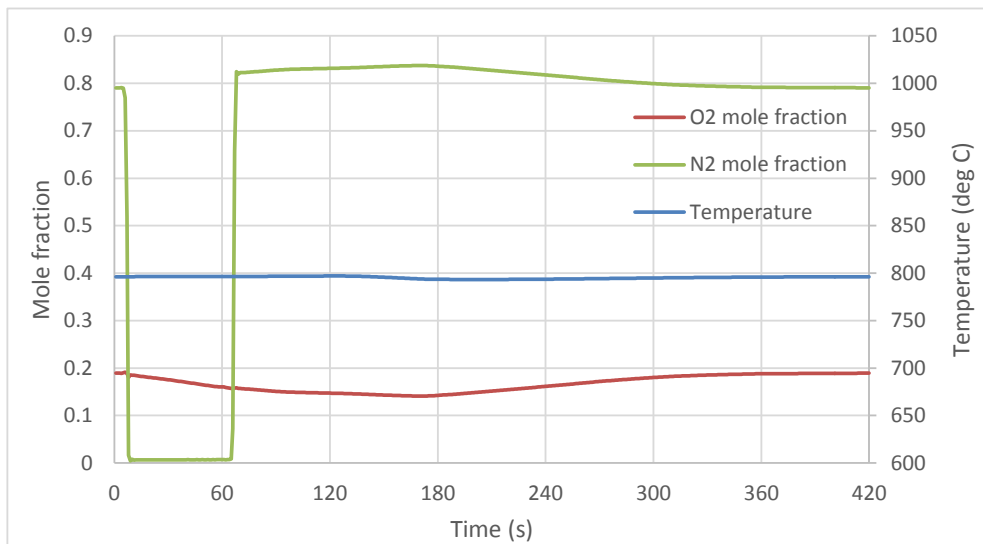

Figure 4: Transient species and temperature profiles at the outlet of the CLOP reactor illustrated in Figure 3. The inlet composition is switched to reduction at 0 s and to air at 60 s according to the specifications in Table 1.

The difference in average O_2 content in the outlet streams during reduction and oxidation (0.5% higher in reduction), the average temperature during both stages (800 °C), the average pressure drops during reduction (0.59 bar) and oxidation (0.8 bar), and the separation efficiency of 98.9% will be used in the power plant simulation presented in Section 5.

4.2. PBCLC reactor

Since there are no equilibrium considerations in the PBCLC system, reactor behavior is simpler than for the CLOP reactor – essentially only a reduction stage with syngas followed by a long oxidation and heat removal stage with depleted air from the CLOP reactors. As explained in the introduction, no heat removal stage with recycled nitrogen is required because the incoming air used for heat removal is pre-heated to 800 °C in the CLOP reactors.

Outlet profiles of species mole fractions and temperature from a PBCLC reactor are shown in Figure 5. The temperature profile shows two distinct dips in the outlet temperature. The first dip is due to the diffuse nature of the heat and reaction fronts, which does not allow for perfect blending between the arriving reaction front and the exiting heat front and the end of the oxidation stage without overheating the oxygen carrier. The second dip is due to a small amount of unconverted Fe_2O_3 remaining at the end of the reduction stage due to slow kinetics.
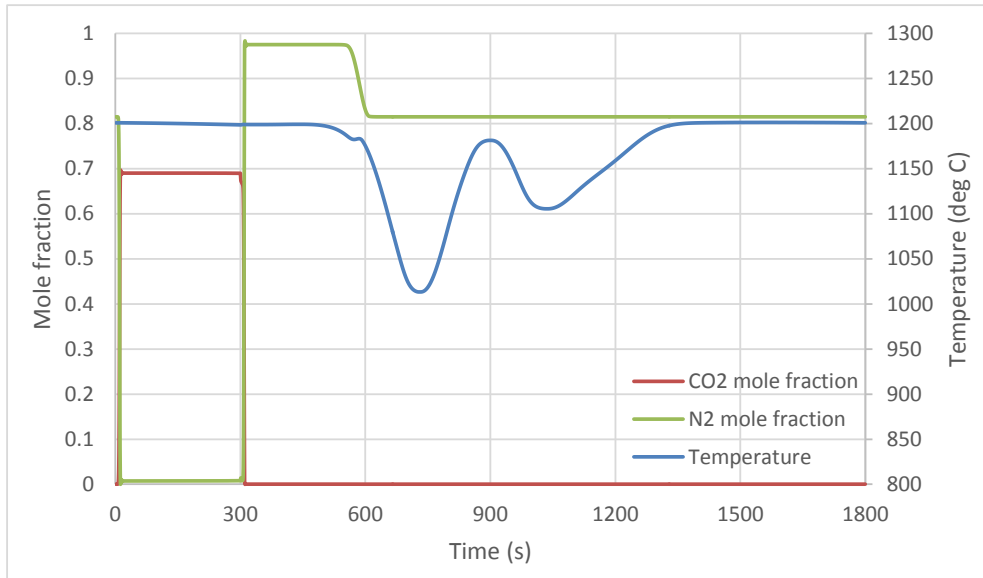
Figure 5: Transient species and temperature profiles at the outlet of the PBCLC reactor. The inlet composition is switched to reduction at 0 s and to oxidation at 300 s according to the specifications in Table 2.

Figure 5 also shows excellent separation between CO_2 and N_2. In this case, however, no delayed outlet switch will be implemented to further improve the CO_2/N_2 separation. The cycles are significantly longer than in the CLOP reactor, implying that the impact of a delayed outlet switch will not be so large. For this PBCLC case, the separation efficiency between the reduction and oxidation outlet gasses amounted to 97%. This means that 3% of the CO_2-rich reduction stage outlet gases end up in the oxidation stage outlet stream and is replaced by the N_2-rich gases from the oxidation stage, thus reducing the CO_2 capture efficiency and CO_2 purity from the process.

Average reactor outlet temperatures during reduction (1200 °C) and oxidation (1165 °C), pressure drops during reduction (0.27 bar) and oxidation (0.77 bar), and a stream separation efficiency of 97% will be used in the power plant simulations presented in the next section.

5. Power plant simulation results

The energy balance resulting from power plant simulation is reported in Table 3. As shown in Figure 2, a syngas booster, consuming ~6.6 MW is necessary in the loop from the gasification system to the CLOP reactors because of pressure loss. Some power consumption is related to the operation of the HGCU station (~2.1 MW), as better detailed elsewhere [19], along with the other consumptions for coal pulverizing and ash handling. Large-size compressor and turbine are necessary at the topping cycle: the compressor has to deliver around 700 kg/s of air to the CLOP system and the turbine exhausts have a similar flow rate. The steam turbine power output is significant compared to the gas turbine power, provided the very large thermal power recovered from the syngas cooling and CO_2 cooling. As for CO_2 compression, the electric consumption is relatively low (~12.7 MW) thanks to the starting pressure of ~16 bar. A CO_2 purification system based on low temperature phase change separation, causing additional consumptions and some CO_2 venting, is however required to increase the CO_2 content from ~94 vol.% (stream 11) to a final purity of 97 vol.%. CO_2 purification unit is calculated considering an auto-refrigerated two-stage separation process as described in [24].

The ultimate efficiency of 45.3% calculated for the assessed power plant is slightly higher than the efficiency of a state-of-the-art IGCC plant without CO_2 capture, for which an efficiency of 45.2% has been calculated with consistent assumptions and calculation methodology [4]. This result is mainly due to: (i) the lack of cryogenic ASU,

causing efficiency losses of about 3.6%-points [4] and (ii) the efficiency gain related to high temperature sulfur removal which can increase the electric efficiency by 2-2.5%-points in a conventional IGCC [3].

An overall CO_2 capture efficiency of 94.92% has been obtained. Emissions are related to CO_2 slip in the CLOP and CLC reactors (3.6% of the inlet carbon), to CO_2 vented from the purification unit (0.8%) and to CO_2 losses from the lock hoppers for coal loading in the gasifier (0.6%). Specific emissions of 34.4 kg_{CO2}/MWh are therefore obtained.

Table 3. Main results of the power plant simulation.

Auxiliaries for gasification plant, MW_e	-11.3
Gas turbine, MW_e	177.1
Steam turbine, MW_e	241.4
Steam cycle pumps, MW_e	-3.2
Auxiliaries for heat rejection, MW_e	-2.9
CO_2 purification and compression, MW_e	-12.7
Balance of plant, MW_e	-1.3
Net power output, MW_e	387.1
Heat input, MW_{LHV}	853.9
Net electric efficiency, %	45.34
CO_2 capture efficiency, %	94.92
CO_2 specific emissions, kg_{CO2}/MWh	34.4

6. Conclusions

The COMPOSITE concept is a promising new configuration for high efficiency power production from solid fuels with inherent CO_2 capture. An integrated gasification combined cycle forms the basis of the COMPOSITE concept, but the combustor is replaced by packed bed chemical looping combustion reactors (PBCLC) and the air separation unit is replaced by chemical looping oxygen production (CLOP) reactors. PBCLC achieves fuel combustion with inherent CO_2 separation and CLOP carries out air separation with minimal energy penalty. In addition, hot gas clean-up is implemented to yield further efficiency gains. The resulting plant efficiency amounts to 45.3% with 95% CO_2 capture efficiency.

In comparison, pre-combustion CO_2 capture from IGCC power plants can achieve 37.7% efficiency and 87% CO_2 avoidance. A CLC-IGCC power plant using an air separation unit can achieve efficiencies ranging from 40.5% to 42% in the best case. In comparison to the CLC-IGCC configuration, the COMPOSITE concept also avoids the need for a nitrogen recycle stream if cheap natural ore is used as oxygen carrier in the PBCLC unit. Furthermore, shared syngas combustion in the CLOP and PBCLC units will reduce strain on the oxygen carrier by limiting the temperature rise in the PBCLC unit. Given all of these advantages, COMPOSITE appears to be a promising concept for further study.

References

[1] X. Zhu, S. Sun, Y. He, Y. Cong, W. Yang, New concept on air separation, Journal of Membrane Science, 323 (2008) 221-224.

[2] B. Moghtaderi, Application of Chemical Looping Concept for Air Separation at High Temperatures, Energy & Fuels, 24 (2010) 190-198.
[3] A. Giuffrida, M.C. Romano, G.G. Lozza, Thermodynamic assessment of IGCC power plants with hot fuel gas desulfurization, Applied Energy, 87 (2010) 3374-3383.
[4] V. Spallina, M.C. Romano, P. Chiesa, F. Gallucci, M. van Sint Annaland, G. Lozza, Integration of coal gasification and packed bed CLC for high efficiency and near-zero emission power generation, International Journal of Greenhouse Gas Control, 27 (2014) 28-41.
[5] H.P. Hamers, M.C. Romano, V. Spallina, P. Chiesa, F. Gallucci, M. van Sint Annaland, Energy analysis of two stage packed-bed chemical looping combustion configurations for integrated gasification combined cycles, Energy, 85 (2015) 489-502.
[6] H.P. Hamers, M.C. Romano, V. Spallina, P. Chiesa, F. Gallucci, M.v.S. Annaland, Comparison on process efficiency for CLC of syngas operated in packed bed and fluidized bed reactors, International Journal of Greenhouse Gas Control, 28 (2014) 65-78.
[7] V. Spallina, F. Gallucci, M.C. Romano, P. Chiesa, G. Lozza, M. van Sint Annaland, Investigation of heat management for CLC of syngas in packed bed reactors, Chem. Eng. J., 225 (2013) 174-191.
[8] S. Cloete, F. Gallucci, M. van Sint Annaland, S. Amini, Gas Switching as a Practical Alternative for Scaleup of Chemical Looping Combustion, Energy Technology, (2016) n/a-n/a.
[9] A. Abad, J. Adánez, F. García-Labiano, L.F. de Diego, P. Gayán, J. Celaya, Mapping of the range of operational conditions for Cu-, Fe-, and Ni-based oxygen carriers in chemical-looping combustion, Chem. Eng. Sci., 62 (2007) 533-549.
[10] F. García-Labiano, J. Adánez, L.F. de Diego, P. Gayán, A. Abad, Effect of Pressure on the Behavior of Copper-, Iron-, and Nickel-Based Oxygen Carriers for Chemical-Looping Combustion, Energy & Fuels, 20 (2005) 26-33.
[11] W. Yang, S. Cloete, J. Morud, S. Amini, An effective reaction rate model for gas-solid reactions with high intra-particle diffusion resistance, International Journal of Chemical Reactor Engineering, 14 (2016) 331-342.
[12] R. Robie, B. Hemingway, Thermodynamic properties of minerals and related substances at 298.15 K and 1 bar pressure and at highe temperatures, in: U.S.D.o.t. Interior (Ed.), 1995.
[13] D.R. Stull, H. Prophet, JANAF Thermochemical Tables, 2nd edition, in: U.S.N.B.o. Standards (Ed.), Washigton D.C., 1971.
[14] S. Patankar, Numerical Heat Transfer and Fluid Flow, Hemisphere Publishing Corporation, United States, 1980.
[15] B.P. Leonard, S. Mokhtari, ULTRA-SHARP Nonoscillatory Convection Schemes for High-Speed Steady Multidimensional Flow, in: NASA TM 1-2568 (ICOMP-90-12), NASA Lewis Research Center, 1990.
[16] D. Toporov, R. Abraham, Gasification of low-rank coal in the High-Temperature Winkler (HTW) process, Journal of the Southern African Institute of Mining and Metallurgy, 115 (2015) 589-597.
[17] D.L. Denton, An update on RTI's warm syngas cleanup demonstration project, in: Gasification Technologies Conference, Washington, DC, 2014.
[18] A. Giuffrida, M.C. Romano, On the effects of syngas clean-up temperature in IGCCs, in: ASME Turbo Expo 2010, Glasgow, UK, 2010.
[19] A. Giuffrida, M.C. Romano, G. Lozza, Efficiency enhancement in IGCC power plants with air-blown gasification and hot gas clean-up, Energy, 53 (2013) 221-229.
[20] P. Chiesa, E. Macchi, A Thermodynamic Analysis of Different Options to Break 60% Electric Efficiency in Combined Cycle Power Plants, Journal of Engineering for Gas Turbines and Power, 126 (2004) 770-785.
[21] A. Giuffrida, S. Moioli, M.C. Romano, G. Lozza, Lignite-fired air-blown IGCC systems with pre-combustion CO2 capture, International Journal of Energy Research, 40 (2016) 831-845.
[22] D. Bonalumi, A. Giuffrida, Investigations of an air-blown integrated gasification combined cycle fired with high-sulphur coal with post-combustion carbon capture by aqueous ammonia, Energy.
[23] S. Moioli, A. Giuffrida, M.C. Romano, L.A. Pellegrini, G. Lozza, Assessment of MDEA absorption process for sequential H2S removal and CO2 capture in air-blown IGCC plants, Applied Energy, 83 (2016) 1452-1470.
[24] S. Campanari, L. Mastropasqua, M. Gazzani, P. Chiesa, M.C. Romano, Predicting the ultimate potential of natural gas SOFC power cycles with CO2 capture – Part B: Applications, Journal of Power Sources, 325 (2016) 194-208.